ACS Macro Letters

Letter

pubs.acs.org/macroletters

Biophysical Characterization of Human Protamine-1 as a Responsive CEST MR Contrast Agent

Nikita Oskolkov,[†,‡] Amnon Bar-Shir,[†,§] Kannie W.Y. Chan,[†,‡,§] Xiaolei Song,[†,‡] Peter C.M. van Zijl,[†,‡] Jeff W.M. Bulte,[†,‡,§] Assaf A. Gilad,*[,†,‡,§] and Michael T. McMahon*[,†,‡]

[†]Russell H. Morgan Department of Radiology and Radiological Science, The Johns Hopkins University School of Medicine, Baltimore, Maryland United States

[‡]F.M. Kirby Research Center for Functional Brain Imaging, Kennedy Krieger Institute, Baltimore, Maryland United States

[§]Cellular Imaging Section and Vascular Biology Program, Institute for Cell Engineering, Baltimore, Maryland United States

Supporting Information

ABSTRACT: The protamines are a low-molecular-weight, arginine-rich family of nuclear proteins that protect chromosomal DNA in germ cells by packing it densely using electrostatic interactions. Human protamine-1 (hPRM1) has been developed as a magnetic resonance imaging (MRI) chemical exchange saturation transfer (CEST) reporter gene, based on a sequence that is approximately 50% arginine, which has a side chain with rapidly exchanging protons. In this study, we have synthesized hPRM1 and determined how its CEST MRI contrast varies as a function of pH, phosphorylation state, and upon noncovalent interaction with nucleic acids and heparin (as antagonist). CEST contrast was found to be highly sensitive to phosphorylation on serine residues, intra- and intermolecular disulfide bridge formation, and the binding of negatively charged nucleotides and heparin. In addition, the nucleotide binding constants (K_{eq}) for the protamines were determined through plotting the molar concentration of heparin versus CEST contrast and compared between hPRM1 and salmon protamine. Taken together, these findings are important for explaining the CEST contrast of existing arginine-rich probes as well as serving as a guideline for designing new genetic or synthetic probes.

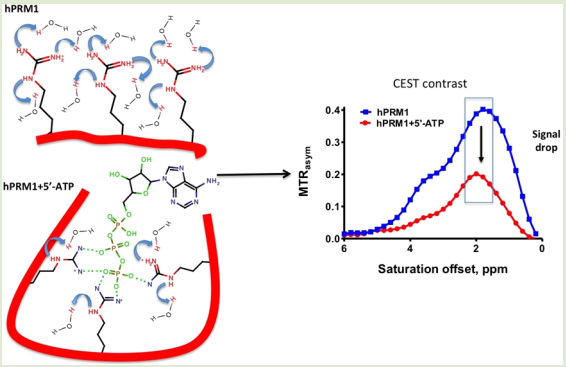

Chemical synthesis of new imaging probes has been critical for obtaining a better understanding of many biological phenomena. Among the different imaging modalities, magnetic resonance imaging (MRI) is unique in that it allows high-resolution anatomical imaging of deep tissue and can provide functional information.[1] MRI has also been shown to be a powerful tool for tracking cells after transplantation, both through nanoparticle approaches[2−6] and through reporter genes.[7−9] This capability can be improved even further through the use of "smart probes".[10,11] The MRI contrast produced by these probes can be enhanced in response to specific cellular changes.

Among the MRI contrast mechanisms, chemical exchange saturation transfer (CEST) stands out, since these probes, often referred to as "contrast agents", can be made of bioorganic molecules. They can be tuned directly, in terms of sensitivity and specificity, by chemical modifications that will modulate the exchange rate of certain protons with water. To detect these chemical modifications, exchangeable protons, which resonate at different resonance frequencies can be selectively "tagged" with a specific radiofrequency pulse, which saturates their magnetization at different resonance frequencies, and read out through the resulting change in water signal. Consequently, this fast growing CEST approach has been utilized to detect pH,[12,13] enzyme activity,[14,15] metal ions,[16] metabolites,[17] reporter genes,[18,19] glycogen and glucose,[20,21] immune responses,[22] tumors,[23] glycosaminoglycan,[24] and even temperature changes.[25] A significant effort has been geared toward designing CEST probes based on polypeptides and proteins, either synthetic[26,27] or genetically encoded.[18,28,29]

When designing a polypeptide or protein-based CEST agent, it is important to take into account interactions of the agent with its environment, which can affect the exchange rate of the probe's protons and, consequently, its MRI contrast. These include the effects of (i) pH, (ii) post-translational modifications such as phosphorylation and disulfide bonds, which change the molecular structure and interaction with other molecules, (iii) protein truncation and degradation, and (iv) interactions with metabolites and other biomolecules of an opposite charge. The protamines are a family of small polypeptides (35−110 amino acids) with between 35 and 70% of their sequence composed of arginine. Naturally occurring protamines can be found in the sperm of different

Received: October 27, 2014
Accepted: December 15, 2014
Published: December 16, 2014

Table 1. Amino Acid Sequence of the Investigated Polypeptides[a]

name	sequence	MW (Da)	Arg content (%)
human protamine-1 (hPRM1)	MARYRCCRSQSRSRYYRQRQRSRRRRRRSCQTRRRAMRCCRPRYRPRCRRH-NH_2	6822	47
salmon protamine sulfate (PS)	PRRRRSSSRPVRRRRRPRVSRRRRRRGGRRRR-OH	4250	65
hPRM1, monophosphate (1p-hPRM1)	MARYRCCRSQSRSRYYRQRQRSRRRRRRSCQTRRRAMRCCRPRYRPRCRRH-NH_2	6902	47
hPRM1, diphosphate (2p-hPRM1)	MARYRCCRSQSRSRYYRQRQRSRRRRRRSCQTRRRAMRCCRPRYRPRCRRH-NH_2	6982	47

[a]Phosphorylated serines in the sequence are highlighted in large, bold font.

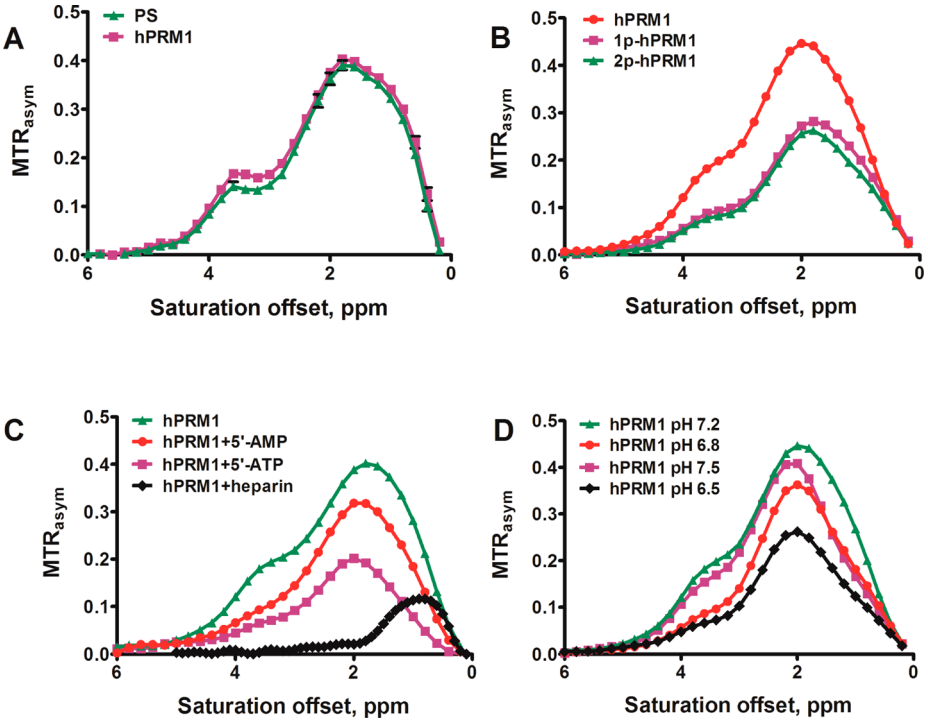

Figure 1. MTR_{asym} of different protamine solutions at various conditions: (A) Comparison of CEST contrast of protamine sulfate and synthetic hPRM1 at the same concentration 0.733 mM in PBS (B_1 = 3.6 μT, T_{sat} = 4 s); (B) Comparison of CEST contrast for mono-, di-, and nonphosphorylated forms of synthetic hPRM1 (B_1 = 3.6 μT, T_{sat} = 4 s); (C) hPRM1 CEST contrast in the presence of negatively charged single nucleotides and polymeric heparin molecules using saturation pulse with B_1 = 3.6 μT, T_{sat} = 4 s; (D) pH dependence of hPRM1 CEST contrast done at B_1 = 3.6 μT, T_{sat} = 4 s.

species, where they condense the spermatid genome into a genetically inactive state through electrostatic interactions to allow delivery to the nucleus of eggs after fertilization.[30] Here, we investigate the CEST contrast of the 51 amino acid long human protamine-1 (hPRM1) protein and its phosphorylated forms (Table 1) after de novo synthesis and purification. These compounds, which are comparable with the shorter, naturally occurring salmon protamine (appears as protamine sulfate, PS), were tested under a variety of conditions and for their ability to interact with several negatively charged biomolecules. In particular, we have used synthetic protamine and its derivatives that were synthesized using microwave-assisted peptide synthesis and investigated its MRI contrast properties.

To date, a majority of the data for polypeptide-based CEST agents have been obtained using either synthetic lysine and arginine-rich peptides[26,31] or PS.[26] Therefore, we first compared the CEST contrast between synthetic hPRM-1 and PS. As can be seen in Figure 1A, both peptides generate CEST contrast with a maximum intensity at a chemical shift 1.8 ppm, where the CEST contrast is associated with the drop in the signal intensity (ΔS) of surrounding water after selective saturation of the exchangeable $-NH_3^+$ protons in the guanidyl side chain of L-arginine at 1.8 ppm. Synthetic hPRM1 produces 35−40% contrast (MTR_{asym}; at 5 mg/mL, 0.733 mM) using a 3.6 μT saturation pulse, which is comparable with PS at the same 0.733 mM concentration (3.11 mg/mL). These findings are in good agreement with previously published data.[29]

For hPRM1, in nature there are multiple sites that are phosphorylated/dephosphorylated during the different stages of spermiogenesis,[32] including serine-9 and serine-13, with this phosphorylation expected to play an important role in the function of the peptide.[33,34] As seen in Figure 1B, mono- (1p-hPRM1) and diphosphorylated (2p-hPRM1) synthetic hPRM1 peptides display at least a 30% drop in CEST contrast, most likely due to interactions between the negatively charge phosphate group and nearby positively charged guanidyl side chain of arginine that reduce the exchange rate. This finding is in accord with previous observations for shorter arginine peptides.[28] The shape of the MTR_{asym} dependence with saturation power (Supporting Information, Figure S9) suggests that the exchange rate is lower for the monophosphorylated peptide; however, due to the poor spectral resolution (the guanidyl protons of the 24 arginine's in the sequence were not resolved), exchange rates were not determined. As expected, the CEST contrast of synthetic hPRM1 is also pH-dependent, with the CEST contrast dropping as the pH decreases below

dx.doi.org/10.1021/mz500681y | ACS Macro Lett. 2015, 4, 34−38

pH 7.2 (Figure 1C). This decrease in contrast was also attributed to a reduction in the exchange rate of the guanidyl protons.

In order to further investigate these observations, we measured the size and secondary structures of the protamine complexes. The hydrodynamic size of the molecule was measured using Dynamic Light Scattering (DLS). DLS measurements of synthetic hPRM1 and PS (6.8 and 4.3 kDa monomers, respectively) indicate that the peptides possess hydrodynamic radii of 4 and 3 nm, respectively (Supporting Information, Table S1), suggesting a molecular weight of about 50 kDa and the presence of tertiary and quaternary structure with at least seven protamine molecules.[35] The data also indicates that hPRM1 in PBS formed larger and more polydisperse particles than PS in PBS. Cysteine-rich domains and inter- and intramolecular noncovalent binding determine the structure of protamines. The formation of bridges between the multiple cysteine residues directs the folding of larger protamines along with hydrogen bonding,[36] with this formation demonstrated by observing a negative result in Ellman's quantitative assay for free sulfhydryl groups. Since PS contains no cysteine at all, the differences between hPRM1 and PS DLS measurements is probably due to the presence of multiple cysteine moieties in the hPRM1 sequence, which form intra- and intermolecular bonds, resulting in larger structures than PS. These features ensure effective protamine binding to nucleic acids[37] forming different sized globular and torroid-like structures.[38] The model proposed by Vilfan[39] for bull protamine consisted of four cysteines forming intramolecular disulfide bonds and the other cysteines participating in intermolecular bonding. Based on the hPRM1 sequence, which contains six cysteine moieties, and our DLS data, we propose a similar model for the potential hPRM1 conformation for isolated protamine molecule or condensed with any negatively charged biomolecule (Figure 2).

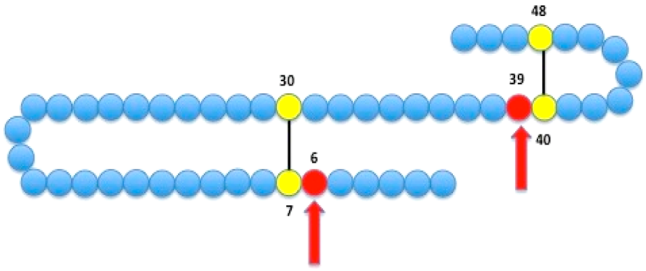

Figure 2. Proposed conformation model of hPRM1 displaying the multiple cysteines involved in intramolecular disulfide bonding (yellow) and intermolecular bonding (red) based on the Vilfan et al., 2004[39] model for bull protamine.

We then acquired a Circular Dichroism (CD) spectrum to study the secondary structure of freshly prepared hPRM1 peptide solution, which displays a clear minimum at 220 nm, indicating that synthetic hPRM1 adopts a structure rich in random coil[40] (Supporting Information, Figure S3A). Since previous studies demonstrated that naturally occurring human protamine could condense with nucleotides and nucleic acids,[41] we investigated the effect of nucleotides on the CEST contrast obtained from hPRM1. DLS studies showed that after addition of 5′-AMP nucleotide at a final concentration of 2.5 mM, synthetic hRPM1 forms nanoparticles with the hydrodynamic size protamine/nucleotide nanocomplex of up to 77 nm, which is comparable with PS/nucleotide nanocomplex sizes. In addition, CD spectra showed that the peptide underwent folding after addition of 5′-AMP nucleotide, which resulted in the secondary structure changing to primarily β-sheet (Supporting Information, Figure S3 and Table S2). This correlates with a modeling study performed by Biegeleisen in 2006[42] and can explain the changes in CEST contrast due to strong interaction of positively charged exchangeable protons of hPRM1 with phosphate group of 5′-adenosine monophosphate (5′-AMP; Figures 1A,D and 3), which also depends on the amount of phosphates in bound nucleotide. The hPRM1 peptide condensed with 5′ adenosine triphosphate (5′-ATP) resulting in more than 3× the reduction in CEST contrast shown by the 5′-AMP:hPRM1 complex (Supporting Information, Figure S6). PS did not display as strong of a binding with 5′-AMP as hPRM1, but was comparable in the case of 5′-ADP and 5′-ATP binding (Supporting Information, Figure S7).

DLS showed that the hPRM1 strongly interacts with a 4000 base pair negatively charged DNA resulting in the formation of large size polydisperse and dense particles. These protamine/DNA nanocomplexes display a drop in CEST contrast to 0% at 1.8 and 3.6 ppm due to protamine's capability of interacting with the phosphates on DNA molecules with high efficiency (Supporting Information, Figure S8) through the exchangeable protons of arginine residues. In addition, it was observed that, upon mixing protamine and DNA together, the mixture turned cloudy, indicating some precipitation. The loss in contrast is much more significant than with the individual nucleic acids AMP and ATP, presumably because all 24 guanidyl groups on protamine could bond to any of the 4000 negative phosphate groups in the DNA strand for these protamine/DNA nanocomplexes.

PS is widely used as an FDA-approved drug to reverse the anticoagulant activity of heparin. In order to check the ability of synthetic protamine to bind the heparin, hPRM1 was mixed with a tiny amount of heparin (0.005−0.1 mg), resulting in a cloudy solution formation, which proves the condensation of heparin into the stable nanoparticles. As a result, the exchangeable protons of arginine interacted with negatively charged sulfates of heparin molecules followed by reduction in CEST contrast at 1.8 ppm (Supporting Information, Figure S4). This hypothesis was also proved by DLS measurement, in which the synthetic hPRM1 showed the capability to interact with heparin molecules resulted in formation of smaller structure nanocomplexes compared to PS/heparin noncovalently bound complexes (Supporting Information, Table S1). This finding suggests that hPRM1 condenses the heparin in another way than PS resulting in the formation of smaller sized nanoparticles with lower polydisperse index probably due to the smaller content of arginines per molecule in the hPRM1 secondary structure, longer primary structure of hPRM1 and the multiple cysteines that form more dense particles compared to PS/heparin particles.

Beyond studying the MRI and binding properties of protamines with heparin, it was also possible to evaluate binding constants (K_{eq}) of heparin−protamine noncovalent complex formation using CEST contrast data of protamines with different amounts of heparin. The heparin-binding constant (K_{eq}) was calculated by recasting the data in the Scatchard plot format and plotting the molar concentration of heparin versus CEST data at 1.8 ppm, which is the normalized value of bounded/unbounded heparin ratio (Supporting Information, Figure S5). The constants obtained from these

dx.doi.org/10.1021/mz500681y | ACS Macro Lett. 2015, 4, 34−38

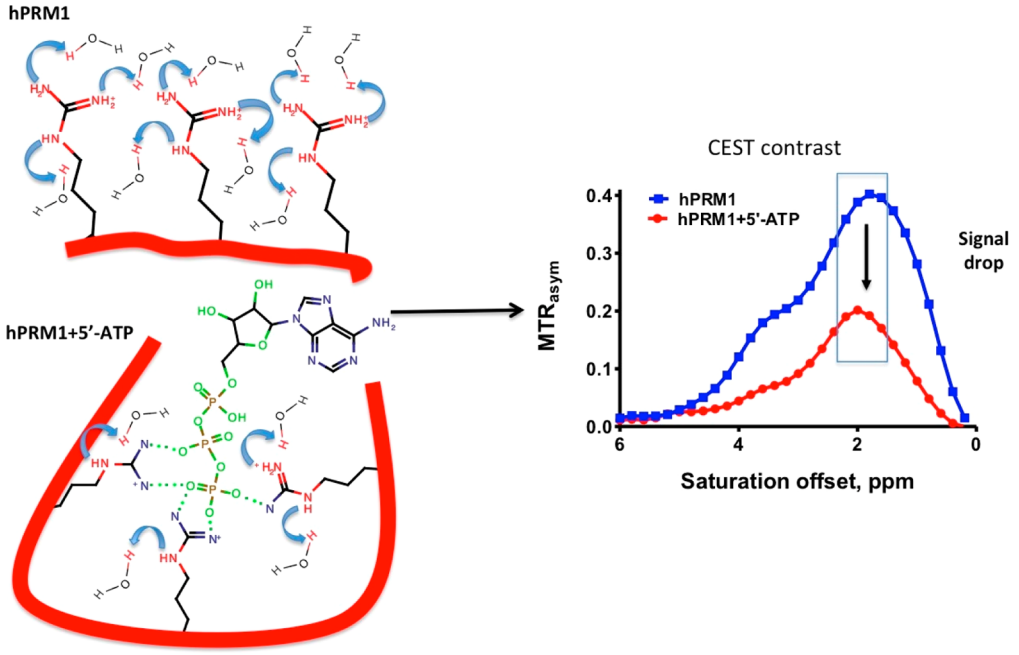

Figure 3. Cartoon of CEST contrast of hPRM1 alone (upper) and complexed with 5′-ATP (lower), which resulted in a decrease of CEST contrast in MTR_{asym}. B_1 = 3.6 μT, T_{sat} = 4 s.

plots are outlined in Supporting Information (Table S1) and in the same range (μM). This data showed that hPRM1 has a better binding affinity for all nucleosides than salmon protamine.

A previous study showed that recombinant hPRM-1 could be expressed in prokaryotic cells after codon optimization as well as in eukaryotic, mammalian cells. Furthermore, the protein synthesized by the cells, which is identical to the protein used in the current study, was detected using CEST MRI in three-dimensional, tissue-like cellular structures.[29] However, inside the cell, many interactions occur, as described in the current study (such as phosphorylation), that reduce the exchange rate and consequently reduce the contrast. The findings from the current study will be useful for engineering mutated isoforms of the hPRM-1 gene that could overcome these obstacles. For example, replacement of the serines which can be phosphorylated or the cysteines involved in disulfide bridges would increase the CEST contrast over the recombinant protein and improve its detection in vivo. It is important to note that CEST MRI has the required sensitivity to detect similar proteins in vivo, in live mouse brain with resolution of approximately 200 × 200 μm.[18,19,43]

In conclusion, hPRM1 was synthesized with a high yield using a microwave synthesizer. This synthetic protein, which generates a CEST contrast comparable to PS, has been used to study the biophysical factors that affect the CEST contrast. Most importantly, it is demonstrated that phosphorylation and interaction with negatively charged metabolites (e.g., ATP, ADP, and AMP) can reduce the CEST contrast via changes in the proton exchange rate and structure. These effects should be taken into consideration when designing new protein-based CEST probes.

■ ASSOCIATED CONTENT

Ⓢ Supporting Information

Additional experimental details and analytical data. This material is available free of charge via the Internet at http://pubs.acs.org.

■ AUTHOR INFORMATION

Corresponding Authors

*E-mail: assaf.gilad@jhu.edu.
*E-mail: mcmahon@mri.jhu.edu.

Notes

The authors declare no competing financial interest.

■ ACKNOWLEDGMENTS

The study was supported in part by R01EB012590, R01EB015031, R01EB015032, and MSCRFII-0042.

■ REFERENCES

(1) Duyn, J. H.; Koretsky, A. P. *Curr. Opin. Neurol.* **2011**, *24* (4), 386−93.
(2) Frank, J. A.; Miller, B. R.; Arbab, A. S.; Zywicke, H. A.; Jordan, E. K.; Lewis, B. K.; Bryant, L. H.; Bulte, J. W. M. *Radiology* **2003**, *228* (2), 480−487.
(3) Evgenov, N. V.; Medarova, Z.; Dai, G. P.; Bonner-Weir, S.; Moore, A. *Nat. Med.* **2006**, *12* (1), 144−148.
(4) Shapiro, E. M.; Skrtic, S.; Sharer, K.; Hill, J. M.; Dunbar, C. E.; Koretsky, A. P. *Proc. Natl. Acad. Sci. U.S.A.* **2004**, *101* (30), 10901−10906.
(5) Heyn, C.; Ronald, J. A.; Mackenzie, L. T.; MacDonald, I. C.; Chambers, A. F.; Rutt, B. K.; Foster, P. J. *Magn. Reson. Med.* **2006**, *55* (1), 23−29.
(6) Ahrens, E. T.; Flores, R.; Xu, H. Y.; Morel, P. A. *Nat. Biotechnol.* **2005**, *23* (8), 983−987.
(7) Cohen, B.; Ziv, K.; Plaks, V.; Israely, T.; Kalchenko, V.; Harmelin, A.; Benjamin, L. E.; Neeman, M. *Nat. Med.* **2007**, *13* (4), 498−503.
(8) Louie, A. Y.; Huber, M. M.; Ahrens, E. T.; Rothbacher, U.; Moats, R.; Jacobs, R. E.; Fraser, S. E.; Meade, T. J. *Nat. Biotechnol.* **2000**, *18* (3), 321−325.

(9) Iordanova, B.; Ahrens, E. T. *Neuroimage* **2012**, *59* (2), 1004−1012.
(10) Moats, R. A.; Fraser, S. E.; Meade, T. J. *Angew. Chem., Int. Ed.* **1997**, *36* (7), 726−728.
(11) Shapiro, M. G.; Westmeyer, G. G.; Romero, P. A.; Szablowski, J. O.; Kuster, B.; Shah, A.; Otey, C. R.; Langer, R.; Arnold, F. H.; Jasanoff, A. *Nat. Biotechnol.* **2010**, *28* (3), 264−U120.
(12) Wu, Y.; Soesbe, T. C.; Kiefer, G. E.; Zhao, P.; Sherry, A. D. *J. Am. Chem. Soc.* **2010**, *132* (40), 14002−3.
(13) Chan, K. W.; Liu, G.; Song, X.; Kim, H.; Yu, T.; Arifin, D. R.; Gilad, A. A.; Hanes, J.; Walczak, P.; van Zijl, P. C.; Bulte, J. W.; McMahon, M. T. *Nat. Mater.* **2013**, *12* (3), 268−75.
(14) Liu, G.; Liang, Y.; Bar-Shir, A.; Chan, K. W.; Galpoththawela, C. S.; Bernard, S. M.; Tse, T.; Yadav, N. N.; Walczak, P.; McMahon, M. T.; Bulte, J. W.; van Zijl, P. C.; Gilad, A. A. *J. Am. Chem. Soc.* **2011**, *133* (41), 16326−9.
(15) Hingorani, D. V.; Randtke, E. A.; Pagel, M. D. *J. Am. Chem. Soc.* **2013**, *135* (17), 6396−8.
(16) Trokowski, R.; Ren, J.; Kalman, F. K.; Sherry, A. D. *Angew. Chem., Int. Ed.* **2005**, *44* (42), 6920−3.
(17) Haris, M.; Cai, K.; Singh, A.; Hariharan, H.; Reddy, R. *Neuroimage* **2011**, *54* (3), 2079−85.
(18) Gilad, A. A.; McMahon, M. T.; Walczak, P.; Winnard, P. T., Jr.; Raman, V.; van Laarhoven, H. W.; Skoglund, C. M.; Bulte, J. W.; van Zijl, P. C. *Nat. Biotechnol.* **2007**, *25* (2), 217−9.
(19) Bar-Shir, A.; Liu, G.; Liang, Y.; Yadav, N. N.; McMahon, M. T.; Walczak, P.; Nimmagadda, S.; Pomper, M. G.; Tallman, K. A.; Greenberg, M. M.; van Zijl, P. C.; Bulte, J. W.; Gilad, A. A. *J. Am. Chem. Soc.* **2013**, *135* (4), 1617−24.
(20) van Zijl, P. C.; Jones, C. K.; Ren, J.; Malloy, C. R.; Sherry, A. D. *Proc. Natl. Acad. Sci. U.S.A.* **2007**, *104* (11), 4359−64.
(21) Walker-Samuel, S.; Ramasawmy, R.; Torrealdea, F.; Rega, M.; Rajkumar, V.; Johnson, S. P.; Richardson, S.; Goncalves, M.; Parkes, H. G.; Arstad, E.; Thomas, D. L.; Pedley, R. B.; Lythgoe, M. F.; Golay, X. *Nat. Med.* **2013**, *19* (8), 1067−72.
(22) Chan, K. W.; Liu, G.; van Zijl, P. C.; Bulte, J. W.; McMahon, M. T. *Biomaterials* **2014**, *35* (27), 7811−8.
(23) Chan, K. W.; Yu, T.; Qiao, Y.; Liu, Q.; Yang, M.; Patel, H.; Liu, G.; Kinzler, K. W.; Vogelstein, B.; Bulte, J. W.; van Zijl, P. C.; Hanes, J.; Zhou, S.; McMahon, M. T. *J. Controlled Release* **2014**, *180*, 51−9.
(24) Ling, W.; Regatte, R. R.; Navon, G.; Jerschow, A. *Proc. Natl. Acad. Sci. U.S.A.* **2008**, *105* (7), 2266−70.
(25) Liu, G.; Qin, Q.; Chan, K. W.; Li, Y.; Bulte, J. W.; McMahon, M. T.; van Zijl, P. C.; Gilad, A. A. *NMR Biomed.* **2014**, *27* (3), 320−31.
(26) McMahon, M. T.; Gilad, A. A.; DeLiso, M. A.; Berman, S. M.; Bulte, J. W.; van Zijl, P. C. *Magn. Reson. Med.* **2008**, *60* (4), 803−12.
(27) Liu, G.; Gilad, A. A.; Bulte, J. W.; van Zijl, P. C.; McMahon, M. T. *Contrast Media Mol. Imaging* **2010**, *5* (3), 162−70.
(28) Airan, R. D.; Bar-Shir, A.; Liu, G.; Pelled, G.; McMahon, M. T.; van Zijl, P. C.; Bulte, J. W.; Gilad, A. A. *Magn. Reson. Med.* **2012**, *68* (6), 1919−23.
(29) Bar-Shir, A.; Liu, G.; Chan, K. W.; Oskolkov, N.; Song, X.; Yadav, N. N.; Walczak, P.; McMahon, M. T.; van Zijl, P. C.; Bulte, J. W.; Gilad, A. A. *ACS Chem. Biol.* **2014**, *9* (1), 134−8.
(30) Sorgi, F. L.; Bhattacharya, S.; Huang, L. *Gene Ther.* **1997**, *4* (9), 961−8.
(31) Goffeney, N.; Bulte, J. W.; Duyn, J.; Bryant, L. H., Jr.; van Zijl, P. C. *J. Am. Chem. Soc.* **2001**, *123* (35), 8628−9.
(32) Chirat, F.; Arkhis, A.; Martinage, A.; Jaquinod, M.; Chevaillier, P.; Sautiere, P. *Biochim. Biophys. Acta* **1993**, *1203* (1), 109−14.
(33) Marushige, Y.; Marushige, K. *J. Biol. Chem.* **1975**, *250* (1), 39−45.
(34) Marushige, Y.; Marushige, K. *Biochim. Biophys. Acta* **1978**, *518* (3), 440−9.
(35) Erickson, H. P. *Biol. Proceed. Online* **2009**, *11*, 32−51.
(36) Englander, S. W.; Mayne, L.; Krishna, M. M. *Q. Rev. Biophys.* **2007**, *40* (4), 287−326.
(37) Carrell, D. T.; Emery, B. R.; Hammoud, S. *Hum. Reprod. Update* **2007**, *13* (3), 313−27.
(38) Arifulin, E. A.; Bragina, E. E.; Zamiatnina, V. A.; Volkova, E. G.; Sheval, E. V.; Golyshev, S. A.; Kintsurashvili, L. N.; Kir'ianov, G. I.; Prusov, A. N.; Poliakov, V. *Ontogenez* **2012**, *43* (2), 143−53.
(39) Vilfan, I. D.; Conwell, C. C.; Hud, N. V. *J. Biol. Chem.* **2004**, *279* (19), 20088−95.
(40) Johnson, W. C., Jr. *Proteins* **1990**, *7* (3), 205−14.
(41) Balhorn, R. *Genome Biol.* **2007**, *8* (9), 227.
(42) Biegeleisen, K. *J. Theor. Biol.* **2006**, *241* (3), 533−40.
(43) Bar-Shir, A.; Liu, G. S.; Greenberg, M. M.; Bulte, J. W. M.; Gilad, A. A. *Nat. Protoc.* **2013**, *8* (12), 2380−2391.